

V. I. Batkin, V. N. Getmanov,  
O. Ya. Savchenko, and R. A. Khusainov\*

UDC 621.384.6

We describe the diagnostics of a plasma jet ejected from the anode hole of a pulsed arc hydrogen plasma source [1-3]. The front part of this source and the grid electrodes are shown in Fig. 1. Grid 1 is at the potential of the plasma, and grid 2 is grounded. Therefore, for a positive plasma potential such a grid diode forms a proton beam [4]. If the diameter of the grids is much larger than the distance between them, the effect of space charge between the grids on the divergence of the beam can be neglected. In a number of cases the effect of the space charge field after the grids can also be neglected if a charge-exchange cell (CC), into which gas is admitted to neutralize the space charge of the beam, is located right after the grids [2, 5]. Therefore, such parallel wire grid electrodes, when combined with a charge-exchange cell, form a beam whose divergence along the wires is determined mainly by the velocity distribution of the protons in the plasma jet [1, 2]. From the phase characteristic of this proton beam it is possible to recover the velocity distribution of protons in the plasma in the direction of the grid wires. It is particularly simple to recover this distribution by analyzing the fast hydrogen atoms formed from these protons in the charge-exchange cell rather than the protons. In this case the particle motion can be considered as free streaming, since the effect of space charge has been eliminated over the whole beam path.

The beam is diagnosed with a system [6] which is nearly the same as those in [7, 8]. In particular, the construction and operation of the secondary emission detectors in [6, 8] are almost identical. The main difference between the system in [6] and those in [7, 8] is that in [6] the experimental data are processed automatically. In addition, in [6] the proton and atomic components of the beam can be analyzed separately with a substantially larger transverse energy resolution. The beam diagnostics system is shown in Fig. 2. Following the charge-exchange cell (CC), the beam passes through a slot detector (SD) and then through two multiwire secondary emission detectors  $D_1$  and  $D_2$  made of gold-plated tungsten wires 30  $\mu\text{m}$  in diameter spaced 1.25 mm apart. The SD contains two orthogonal pairs of graphite collimators whose positions can be adjusted to within 0.1 mm, and gap widths to within  $\pm 20 \mu\text{m}$ , thus permitting the selection of any portion of the beam for analysis. By applying a potential difference between a pair of collimators the  $\text{H}^+$  ions can be deflected to ensure the separate analysis of  $\text{H}^0$  and  $\text{H}^+$ . The collimator plates extend 18 mm along the beam, and are ground off at an angle of  $5 \cdot 10^{-2}$  rad to make the system insensitive to the failure of the beam axis to coincide with the symmetry axis of the detector. The gap width and position are monitored by capacitive- and potentiometer-type sensors respectively. The part of the beam thus defined is analyzed by multiwire probes having a total transmittance of 96%. The system ensures separate analysis of the  $\text{H}^0$  and  $\text{H}^+$  beams in two projections simultaneously, and a determination of the parameters of the angular divergence to within  $10^{-4}$  rad.

To determine the velocity distribution in the plasma jet the slot of the first collimator, which is perpendicular to the electrode wires, is opened to 150-200  $\mu\text{m}$ , and the other slot is opened to 10 mm. The beam defined by the first slot is analyzed by the probe wires which are perpendicular to those of the grid electrodes. The probe electronics make it sensitive to 1 pC per wire for a dynamic range of  $\sim 6000$  pC. The drift of the signal resulting from leakage in the elements of the analog memory is 8 pC/sec. The probe wires can be biased to  $\pm 100$  V, and the beginning of the integration of the current can be gated. The experiment was automated by using an "Elektronika-100 I" computer and a multichannel analog-digital interface. To increase the accuracy, the final calculations were carried out with average values and dispersions of the beam profile obtained by averaging over a group consisting usually of 20-30 events. For convenience the computer was programmed to determine

\*Deceased.

Novosibirsk. Translated from Zhurnal Prikladnoi Mekhaniki i Tekhnicheskoi Fiziki, No. 6, pp. 30-36, November-December, 1982. Original article submitted October 21, 1981.

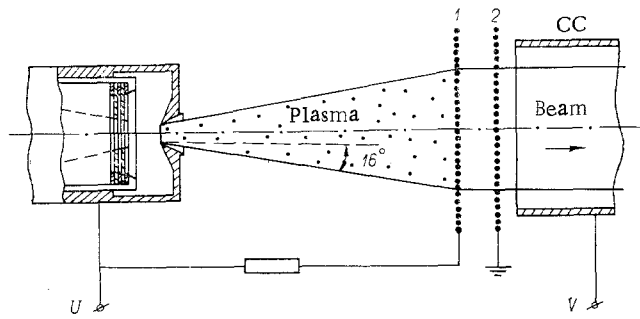


Fig. 1

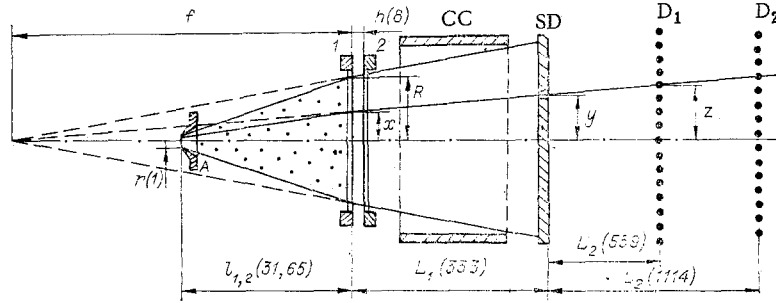


Fig. 2

the beam profile with each event on the storage oscillograph screen. The beam profile obtained is integrated numerically and found to be approximately Gaussian. Data accumulation is at the rate of 0.2 Hz with running averaging, and 300 Hz without averaging.

In the version of the arc source under investigation [3] the plasma is ejected onto the first grid in the form of a jet with a divergence of  $\sim 16^\circ$ . This indicates that the longitudinal component of the particle velocity  $v_{\parallel}$  is several times larger than the transverse component. If the velocity  $v_{\parallel}$  has a small dispersion, and the plasma is free streaming, then for  $l \gg r$  the particles which strike grid 1 at distances  $x$  from the center such that  $x \gg r$  (Fig. 2) have a transverse velocity  $v_x \approx (x/l)v_{\parallel}$ , where  $l$  is the distance from the anode A to grid 1, and  $r$  is the radius of the anode hole. Thus, at the first grid the transverse velocities of the particles increase linearly with their distance from the center, and particles accelerated by a potential  $U$  to a velocity  $v_U$  will have a virtual focus at a distance

$$f \approx (x + 2hv_x/v_U)v_U/v_x - h,$$

from the first grid, where  $h$  is the distance between grids. Therefore, the part of the beam passing through the collimator slot at a distance  $y$  from the center of the beam falls on a probe wire at a distance

$$z = (L_1 + L_2 + f)y/(L_1 + f), \quad (1)$$

from the center of the beam, where  $L_1$  is the distance between the first grid and the collimator slot, and  $L_2$  is the distance between the collimator slot and the probe. It follows from Eq. (1) that

$$x/v_x \approx (z/y - L_1/L_2 - h/L_2 - 1)L_2 \sqrt{m_p/2eU}. \quad (2)$$

Equation (2) can be used for an experimental determination of  $\bar{v}_x/x$ .

In the first version the jet was studied at a distance  $l_1 = 31$  mm from the anode hole. The grid electrodes were 52 mm in diameter and 8 mm apart, the wires of the first grid were 28  $\mu$ m in diameter and 136  $\mu$ m apart, and the wires of the second grid were 0.1 mm in diameter and 0.5 mm apart. Figure 3 shows the dependence of  $z_1$ , the coordinate of the center of the profile of the part of the beam defined by the SD at detector  $D_1$ , on  $y_1$ : the coordinate of the SD slot for arc currents of 140, 220, 330, 370, and 400 A (points 1-5 respectively). The beam particles had an energy of 10.3 keV, the delay time between the triggering of the arc and the triggering of the gas valve was 600  $\mu$ sec, and the pressure at the valve was

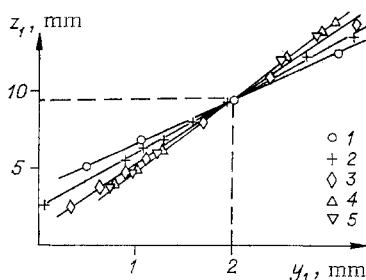


Fig. 3

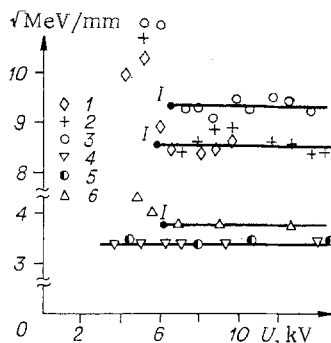


Fig. 4

TABLE 1

Arc current, A	Delay time of triggering of arc, $\mu$ sec	$(\bar{v}_x/x) \cdot \sqrt{m_p/2}$ , $\sqrt{\text{MeV}/\text{mm}}$	Longitudinal energy, eV	Note
140	600	$8.60 \pm 0.30$	$71 \pm 4$	Version 1
165	600	$8.60 \pm 0.12$	$71 \pm 3$	
190	600	$9.30 \pm 0.30$	$83 \pm 5$	
190	600	$3.50 \pm 0.10$	$50 \pm 2$	Version 2 The relative error is indicated in each version. The absolute error, related to the inaccuracy in the determination of the position of the beam center, does not exceed 25%.
190	900	$3.45 \pm 0.10$	$49 \pm 2$	
220	600	$3.67 \pm 0.03$	$56 \pm 1$	
220	900	$3.47 \pm 0.03$	$51 \pm 1$	
270	600	$3.75 \pm 0.05$	$62 \pm 2$	
270	900	$3.47 \pm 0.03$	$51 \pm 1$	
330	600	$4.30 \pm 0.15$	$78 \pm 5$	
330	900	$3.95 \pm 0.05$	$66 \pm 2$	
400	600	$4.60 \pm 0.20$	$89 \pm 8$	
400	900	$4.20 \pm 0.20$	$74 \pm 5$	
190	600		$41.6 \pm 0.9$	The result of computer processing using Eqs. (5)-(7). The absolute error is indicated.

0.25 MPa. The coordinates  $(z_0, y_0)$  of the center of the beam were determined from the intersection of the straight lines in Fig. 3. Then  $y = y_1 - y_0$  and  $z = z_1 - z_0$  were found, and Eq. (2) was used to determine  $\bar{v}_x/x$ . Figure 4 shows the values of  $(\bar{v}_x/x) \sqrt{m_p/2}$  calculated for various values of the potential  $U$  for arc currents of 140, 190, and 200 A (points 1-3). The slot was fixed 6.8 mm from the center of the beam. As can be seen from Fig. 4,  $(\bar{v}_x/x) \sqrt{m_p/2}$  is constant down to point 1, and then increases sharply because of the entrance of the plasma into the intergrid gap [2, 4]. In this case the calculated value is not a parameter related to the spread of the plasma jet, since it is determined mainly by the curvature of the boundary of the plasma entering the intergrid gap. Therefore, the region to the left of point 1 cannot be used to determine the plasma spread parameter. This imposes restrictions on the measurements of  $\bar{v}_x/x$  for large arc currents and a chosen distance between the first grid and the anode hole: for arc currents of more than 250 A point 1 is displaced into the range of potentials above 15 kV. Therefore, to measure  $\bar{v}_x/x$  for a wider range of arc currents, the grid electrodes were separated from the anode hole by a distance  $l_2 = 65$  mm. In addition, detector  $D_2$  was used to increase the accuracy of measurement.

Figure 4 shows some of the values of  $(\bar{v}_x/s)\sqrt{m_p/2}$  calculated from the experimental data of the second version for arc currents of 190, 220, and 270 A (points 4-6 respectively). Curves similar to those of Fig. 4, but not shown on it, were obtained in the second version for slots from 2 to 8 mm from the center. The curves were used to determine the average values of  $(\bar{v}_x/s)\sqrt{m_p/2}$  for various arc currents. The data obtained, together with some results from the first version, are listed in Table 1, which shows that with increasing arc current the value of  $(\bar{v}_x/x)\sqrt{m_p/2}$  increases monotonically from 3.4 to 4.6  $\sqrt{\text{meV}/\text{mm}}$ , and the values of  $(\bar{v}_x/x)\sqrt{m_p/2}$  in identical plasma jets (arc current 190 A) in the first version of the experiment, in agreement with the assumption of the free streaming of protons in the plasma, are approximately  $l_2/l_1$  times larger than in the second version. For free streaming the product  $(\bar{v}_x l/x)^2(m_p/2)$ , which is the longitudinal energy of protons in the plasma jet, does not vary with the distance from the anode hole. The values of this parameter for various conditions of arc discharge are listed in Table 1.

The observed linear dependence of the average radial proton velocity on the distance from the axis in a cross section of the plasma jet confirms the assumption of free streaming of plasma protons in this source [7], which makes it possible to estimate the upper limit of the average energy of the transverse motion of the protons. This energy does not exceed  $(\bar{v}_x R/x)^2(m_p/2)$ , where R is the radius of the plasma jet at the place  $\bar{v}_x/x$  is measured. Estimates using this formula show that the upper limit of the average energy of the transverse motion of the protons in the jet varies from 1.8 to 3.4 eV for currents in the range 190-400 A. These values can evidently be identified with the upper limit of the transverse temperature of protons at the exit from the anode hole, and can be used to estimate the jet temperature, since the temperature T in a cross section of a jet of radius R for free streaming is related to the anode temperature  $T_0$  by the expression

$$R^2 T \simeq r^2 T_0. \quad (3)$$

Therefore

$$T \simeq T_0(r/R)^2 < (\bar{v}_x r/x)^2(m_p/2). \quad (4)$$

Thus, the upper limit of the transverse temperature is related to the experimentally determinable quantity  $\bar{v}_x/x$  and the radius r of the anode hole. Estimates with (4) indicate that at a distance of 65 mm from the anode hole the proton temperature in the jet decreases to a few meV. This effect was observed experimentally by measuring the thermal spread of beam particles in the collimator plane. Since this plane is quite far from the plane of the source exit grid, the transverse temperature in the beam was determined by measuring the current density distribution  $I(x, \varphi)$  of the  $H^0$  component of the beam in phase space whose parameters are the coordinate x and the angle of divergence  $\varphi = v_x/v_U$ . The experimentally measurable quantity  $I(y, \varphi)$  in the SD plane was transformed into the required distribution function  $I(x, \varphi)$  in the plane of the source grid by the formula corresponding to free streaming of the particles

$$I(x, \varphi) = I(y - \varphi L_1, \varphi). \quad (5)$$

$I(y, \varphi)$  was determined by scanning the beam over the y coordinate with a narrow gap of the SD, and at each position of the gap measuring, in the automated regime, the average beam profile, represented by signals from the detector wires, and also the position and width of the SD gaps and the proton source current. A potential difference was maintained between the SD plates to ensure the deflection of the charged components of the beam beyond the detector aperture. The thermal spread  $\alpha$  of the beam was so small ( $\alpha \leq 10^{-3}$  rad) that in order to determine the profile shape from nonzero signals from two to four wires it was necessary to combine measurements in which the positions of the SD slot differed by  $\sim 1/3$  the distance between detector wires. Taking account of the fact that the average radial velocity of protons in a cross section of the beam varies linearly with their distance from the center of the beam, and that the region scanned was limited to the central part of the beam, the measurable distribution can be approximated by a simple model function of the form

$$I(y, z) = N \exp[-B(z - ky - c)^2], \quad (6)$$

where the parameters B, k and c are determined in the course of fitting it to the experimental data. Then the distribution function in phase space (y,  $\varphi$ ) is determined:

$$I(y, \varphi) = N \exp[-BL_2^2(\varphi - (k-1)y/L_2)^2], \quad (7)$$

which, after transformation by formula (5), becomes

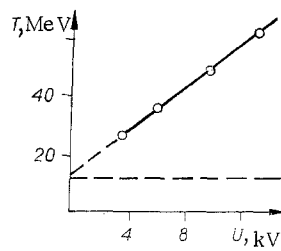


Fig. 5

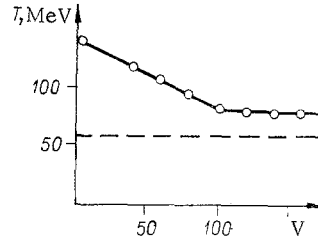


Fig. 6

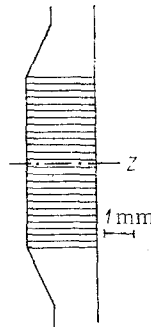


Fig. 7

$$I(x, \varphi) = N \exp [-(E/T)(\varphi - \kappa x)^2], \quad (8)$$

$$T = (E/B)[L_2 - (k-1)L_1]^{-2}, \quad \kappa = (k-1)/[L_2 - (k-1)L_1],$$

where  $T$  is the transverse temperature of the beam protons at the source exit,  $E$  is their longitudinal energy, and  $\kappa x = \varphi$ .

Using the method described, the experimental results obtained in the second version for energies from 3 to 15 keV and an arc current of 190 A were processed by computer to determine the initial transverse temperature in the beam and  $\bar{v}_x/x$ . The difference between the value of the longitudinal energy (41.6 eV, Table 1) corresponding to the value obtained for  $\bar{v}_x/s$ , and the value (50 eV) obtained under these same conditions by using Eq. (2), lies within the limits of absolute error (25%) of the determination of the latter. This error is related to the inaccuracy of the determination of the position of the center of the beam, and is due to the error in determining the  $y$  and  $z$  coordinates (Fig. 2).

Figure 5 shows the values obtained for the transverse temperature in the plane of the beam-source grid in these same experiments. The strong dependence of the beam temperature on the potential of grid 1 indicates the presence of factors which increase the thermal spread of the beam after its formation. The results presented give an upper estimate of 24 meV for the transverse temperature of the ions of the plasma jet near the first grid. The temperature determined in this way is of the same order of magnitude as the upper limit of 12 meV obtained by assuming free streaming of the plasma protons. A more accurate determination of the transverse temperature of the plasma protons requires eliminating or taking account of the factors which increase the effective transverse temperature of the beam particles. In particular, the linear increase of the effective temperature in Fig. 5 may possibly result from the wires of the grid electrodes not being perpendicular to the wires of the secondary emission detector. Another effect is related to the fact that the gas

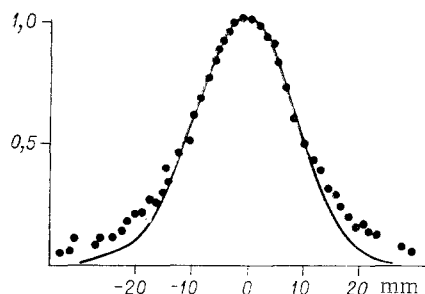


Fig. 8

target is very extended (30 cm), and in incomplete charge compensation the neutral component may include atoms formed in regions with different radial divergences. The result of this effect is proportional to the distance from the beam axis. But no strong dependence of the beam temperature on the distance from its axis was observed, and this confirms the previous assumption that space charge in the charge-exchange cell has no effect. Finally, nonstationary plasma processes in the charge-exchange cell may affect the beam temperature. The observed dependence of the beam temperature on the potential of the charge-exchange cell indicates the presence of such processes. The form of this dependence varies with the beam energy, the arc current, and the density of the gas target, but in all cases the beam temperature decreased with increasing potential  $V$  of the charge-exchange cell up to 180 V, and then the  $T(V)$  curve reaches a plateau for large positive potentials of the cell. In this case there are no irregular modulations of the beam current such as were observed for small positive potentials of the cell. Figure 6 shows an example of such a relation in the first version for an intergrid potential of 10 kV and an arc current of 270 A. The increase in the effective temperature of the beam particles was also investigated for the charge-exchange neutralization of a beam of protons into fast hydrogen atoms. For particle energies in the range 5-15 keV it turned out to be no larger than a few meV [9]. This result does not contradict the data of [10], where it was found that for 10 keV particles the effective temperature was increased by  $2.5 \pm 0.7$  meV in the charge-exchange neutralization of  $H^+$  into  $H^0$ .

The diagnostics of the plasma jet confirmed the assumption of Roslyakov [7] of the free streaming of protons in a plasma jet. In this case the transverse phase characteristics of the jet protons at a sufficiently large distance  $l$  from the anode hole are determined only by the longitudinal energy  $E$  of the protons and the radius  $r$  of the anode hole: the transverse temperature in a jet  $T \approx E(r/l)^2$ , and the average energy of the radial motion of protons at a distance  $x$  from the jet axis  $E_x \approx E(x/l)^2$ . Therefore, Table 1, which lists the values of  $E$  for various operating conditions of the plasma arc source, makes it possible to determine the phase characteristics of the proton beam formed at a distance  $l$  from the anode. It is possible, for example, by placing the grid electrodes near the anode hole, to obtain a beam with a high current density and a relatively small divergence, if the proton beam is formed from the central part of the plasma jet. Figure 7 shows grid electrodes which should form a practically parallel beam of protons from stationary protons. A calculation by the method of [11] shows that the outer current tubes in the space-charge regime are deflected no more than  $2 \cdot 10^{-3}$  rad from the beam axis. Figure 8 shows the density distribution in a beam of particles formed by these grid electrodes at a distance of 920 mm from them. It follows from Fig. 8 that the average transverse energy of particles of this beam is  $\approx 3$  eV. The energy of the protons in the beam is 15.4 keV, and the current is 200 mA. The radius of the beam at the exit from the electrodes is 2.5 mm, and the distance between the first grid and the anode hole is 13 mm. The value of  $E$  is  $\approx 70$  eV, and therefore the energy of particles at the edge of the beam is  $E_x \approx 70(2.5/13)^2$  eV = 2.6 eV. As expected, it turned out to be close to the average transverse energy of the beam particles.

#### LITERATURE CITED

1. G. I. Dimov, Yu. G. Kononenko, et al., "Production of high-intensity hydrogen ion beams," *Zh. Tekh. Fiz.*, **38**, 997 (1968).
2. G. I. Dimov, G. V. Roslyakov, and O. Ya. Savchenko, "Formation of a stream of ions and neutral atoms from a plasma of a pulsed arc source," Preprint Inst. Nucl. Phys., Siberian Branch, Academy of Sciences of the USSR, Novosibirsk (1967).
3. G. I. Dimov and G. V. Roslyakov, "Pulsed charge-exchange source of negative hydrogen ions," *Prib. Tekh. Eksp.*, No. 1 (1974).

4. O. Ya. Savchenko, "Formation of intense ion beams by grid electrodes," in: Proc. Second All-Union Conf. on Charged Particle Accelerators, Vol. 1 [in Russian], Moscow (1970).
5. O. Ya. Savchenko, "Production of ions by ionization of neutral particles on a helium gas target," Zh. Tekh. Fiz., 40, 305 (1970).
6. V. N. Getmanov and V. I. Batkin, "Automated system for the diagnostics of a beam of hydrogen ions," in: Problems of Atomic Science and Engineering, Series TFE [in Russian], Nos. 2-4 (1979).
7. G. V. Roslyakov, "Transducer for measuring transverse velocities of ions of a plasma emitter," Prib. Tekh. Eksp., No. 2 (1981).
8. A. S. Brus, A. I. Velikov, et al., "Ion beam monitor," Prib. Tekh. Eksp., No. 3 (1981).
9. V. I. Batkin, V. N. Getmanov, et al., "Effect of gas targets on the angular divergence of a beam of fast hydrogen atoms," Eighth All-Union Conf. on the Physics of Electron and Atomic Collisions. Abstracts of Papers [in Russian], Leningrad (1981).
10. A. B. Wittkower and H. B. Gilbody, "A study of the charge neutralization of fast  $\text{Ne}^+$ ,  $\text{Ar}^+$ , and  $\text{Kr}^+$  ions during passage through gaseous targets," Proc. Phys. Soc., 90, 353 (1967).
11. V. Ya. Ivanov and V. P. Il'in, "Solutions of mixed boundary-value problems for Laplace's equation by the method of integral equations," in: Standard Programs for Solving Mathematical Physics Problems [in Russian], Computing Center, Siberian Branch, Academy of Sciences of the USSR, Novosibirsk (1975).

#### DISPERSION OF A PLASMA CLUSTER OVER A LESS DENSE PLASMA BACKGROUND

Yu. A. Berezin and P. V. Khenkin

UDC 533.9

A number of theoretical reports have been devoted to a study of the question of the motion of plasma clusters over a plasma background (see [1-3], for example). The influence of finite conductivity (Coulomb and anomalous) on cluster motion and magnetic field growth is investigated in the present report. The problem of expansion of a plasma cylinder into a rarefied plasma is modeled numerically. Since in a first approximation we are interested not in the structure of the shock wave but in the process of plasma interaction with the magnetic field and the influence on this interaction of ion-sonic and beam instabilities, we chose the model of two-fluid hydrodynamics, which is simpler than the hybrid model.

We consider the nonsteady axisymmetric problem, when all the unknown functions are functions of the radius  $r$  and time  $t$  and the magnetic field has only a  $z$  component, directed along the axis of the cylindrical coordinate system:  $\mathbf{H} = \{0, 0, H\}$ . Then the system of equations of two-fluid magnetohydrodynamics [4] for the cylindrical case in Eulerian coordinates can be written in the form

$$\begin{aligned}
 \left(\frac{\partial}{\partial t} + u \frac{\partial}{\partial r}\right)n &= -n \left(\frac{\partial u}{\partial r} + \frac{u}{r}\right), \quad (m_i + m_e)n \left(\frac{\partial}{\partial t} + u \frac{\partial}{\partial r}\right)u = \\
 &= -\frac{\partial}{\partial r} \left(nT_i + nT_e + \frac{H^2}{8\pi}\right) + \frac{c^2 m_i m_e}{16\pi^2 e^2 (m_e + m_i)n} \frac{1}{r} \left(\frac{\partial H}{\partial r}\right)^2, \\
 \left(\frac{\partial}{\partial t} + u \frac{\partial}{\partial r}\right)H &= -\left(\frac{\partial u}{\partial r} + \frac{u}{r}\right)H - \frac{c^2 m_e m_i}{4\pi e^2 (m_e + m_i)} \left(\frac{\partial}{\partial r} + \frac{1}{r}\right) \times \\
 &\times \left(\frac{\partial}{\partial t} + u \frac{\partial}{\partial r} + \frac{u}{r}\right) \left(\frac{1}{n} \frac{\partial H}{\partial r}\right) - \frac{c}{e} \left(\frac{\partial}{\partial r} + \frac{1}{r}\right) \frac{R_\Phi}{n}, \\
 \frac{3}{2} n \left(\frac{\partial}{\partial t} + u \frac{\partial}{\partial r}\right)T_e &= -nT_e \left(\frac{\partial u}{\partial r} + \frac{u}{r}\right) - \left(\frac{\partial}{\partial r} + \frac{1}{r}\right)q_{er} + Q_e, \\
 \frac{3}{2} n \left(\frac{\partial}{\partial t} + u \frac{\partial}{\partial r}\right)T_i &= -nT_i \left(\frac{\partial u}{\partial r} + \frac{u}{r}\right) - \left(\frac{\partial}{\partial r} + \frac{1}{r}\right)q_{ir} + Q_i,
 \end{aligned} \tag{1}$$

Novosibirsk. Translated from Zhurnal Prikladnoi Mekhaniki i Tekhnicheskoi Fiziki, No. 6, pp. 37-40, November-December, 1982. Original article submitted October 8, 1981.